# A free-electron model for the Dirac bands in graphene

G. S. Kissinger and S. Satpathy

Phys. Rev. B **94**, 205126 — Published 16 November 2016

DOI: 10.1103/PhysRevB.94.205126

# A free-electron model for the Dirac bands in graphene

G. S. Kissinger and S. Satpathy
*Department of Physics & Astronomy, University of Missouri, Columbia, MO 65211, USA*
(Dated: August 19, 2016)

We present a new method for describing the electronic structure of graphene, by treating the honeycomb lattice as an arrangement of criss-crossing one-dimensional quantum wires. The electrons travel as free particles along the wires and interfere at the three-way junctions formed by the carbon atoms. The approach produces the linearly dispersive Dirac band structure as well as the chiral pseudo-spin wave functions. When vacancies are incorporated, the model reproduces the well known zero mode states.

PACS numbers: 73.22.Pr

Graphene, a two-dimensional honeycomb lattice of carbon atoms, has been the subject of enormous interest in condensed matter physics in recent years on account of its interesting electronic properties, such as the linearly dispersive Dirac bands and their associated chiral wave functions, which in turn lead to a variety of intriguing phenomena such as the Klein paradox, the half-integer quantum Hall effect, Berry phase effects, and many others.[1–3] The band structure of graphene is typically described by the tight-binding model[4], by density-functional band calculations[5], or by solving the Schrödinger equation for the hexagonally periodic potential[6], all of which produce the linear energy dispersion centered around the Brillouin zone corners $K$ and $K'$. Here, we describe a new way of obtaining the graphene band structure, where electrons propagate as one-dimensional (1D) waves along the bonds of the honeycomb lattice. The characteristic linear dispersion of the electron states as well as the chirality of the pseudo-spin wave functions are produced by interference of the wave functions at the three-way junctions formed by the carbon atoms.

In our treatment, graphene is considered as a hexagonal lattice of 1D wires, so that the Schrödinger equation in each wire has simply the plane wave solution

$$\psi_i = a_i e^{i\bar{k}x_i} + b_i e^{-i\bar{k}x_i}, \tag{1}$$

where the electron energy is $E = (2m)^{-1}\hbar^2\bar{k}^2$, $x_i$ is the position defined along the $i$-th wire ($0 \le x_i \le a$, $a$ being the C-C bond length), and $m$ is the effective mass of the electron in the graphene lattice. The wave function on the entire lattice can be generated from wave functions on three wires, which constitute the unit cell of the crystal, using the Bloch symmetry

$$\psi_i = e^{i\vec{k}\cdot\vec{T}}\psi_j, \tag{2}$$

where wires $i, j$ are connected by the lattice translation vector $\vec{T}$ and $\vec{k}$ is the Bloch momentum, so that for a given Bloch momentum, we have just six unknowns $(a_i, b_i, i = 1, 2, 3)$ that describe the full solution on the entire lattice. The wave functions must satisfy the standard boundary conditions at the junctions. The continuity of the wave function and the conservation of the particle current lead to the conditions

$$\psi_1 = \psi_2 = ... = \psi_n, \tag{3}$$

$$\sum_{i=1}^{n} d\psi_i/dx_i = 0, \tag{4}$$

where $i$ labels the $n$ branches forming the junction ($n = 3$ for graphene), all coordinates in the derivative $\psi_i' = d\psi_i/dx_i$ point either away or towards the junction by convention, and $\psi_i$ and $\psi_i'$ are evaluated at the junction points. These boundary conditions were originally developed[7] for the study of conjugated molecules and have been used to study transmission through quantum nanostructures[8,9] as well as through photonic molecules.[10] Here we extend the method for the first time to study electronic band structure in crystalline solids, using graphene as the example.

For transmission through a three-way junction (Fig. 1), these boundary conditions readily lead to the scattering matrix

$$S = \begin{pmatrix} -1/3 & 2/3 & 2/3 \\ 2/3 & -1/3 & 2/3 \\ 2/3 & 2/3 & -1/3 \end{pmatrix}, \tag{5}$$

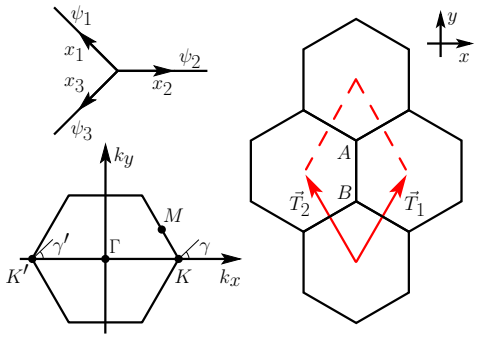


FIG. 1. (Color online) Transmission through a single three-way junction (*top left*). There are two such junctions, A and B, in the unit cell corresponding to the two sublattices (*right*), while the (*bottom left*) shows the Brillouin zone of the graphene lattice.

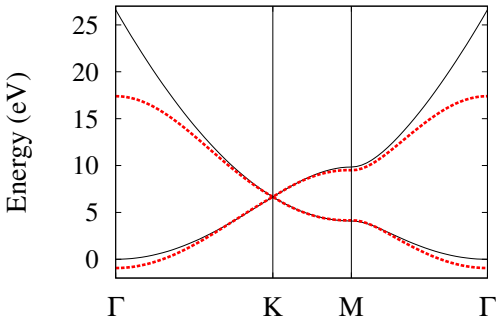


FIG. 2. (Color online) Energy dispersion for graphene obtained from Eq. (12) (black line) compared with the results from the third nearest-neighbor tight-binding model[5] (red dashed line).

which relates the amplitudes of the incoming to the outgoing waves, viz., $\vec{a} = S\vec{b}$, where $\vec{a} = (a_1, a_2, a_3)$ and $\vec{b} = (b_1, b_2, b_3)$. Turning now to the hexagonal graphene lattice, we get three equations for each of the two junctions (corresponding to the two sublattices) in the unit cell from the boundary conditions, viz., two equations from Eq. (3) and one from Eq. (4). These six linear equations may be written in the matrix form

$$M\vec{X} = 0, \tag{6}$$

$$M(\bar{k}, \vec{k}) = \begin{pmatrix} I & -S \\ I & -\lambda B^{-1} S B \end{pmatrix}, \tag{7}$$

where $\vec{X} = (a_1, a_2, a_3, b_1, b_2, b_3)$, $I$ is the 3×3 unit matrix, $\lambda = e^{-2i\bar{k}a}$, and $B$ is the Bloch factor matrix

$$B = \begin{pmatrix} e^{-i\vec{k}\cdot\vec{T}_2} & 0 & 0 \\ 0 & e^{-i\vec{k}\cdot\vec{T}_1} & 0 \\ 0 & 0 & 1 \end{pmatrix}, \tag{8}$$

$\vec{T}_1, \vec{T}_2$ being the two primitive translation vectors connecting the second-neighbor atoms as indicated in Fig. 1. For a non-trivial solution for the wave function, the determinant of $M$ must vanish, viz.,

$$\det M(\bar{k}, \vec{k}) = 0. \tag{9}$$

The determinant can be readily evaluated to yield the result, which is of the form $\det M = \sin(\bar{k}a) \times D$. It can be shown that equating the first term to zero does not produce any non-trivial solutions except at the Γ point, where it coincides with one of the solutions obtained from the second term. Thus, all distinct solutions are contained in the second term, viz.,

$$D = 9\cos^2(\bar{k}a) - 3 - f(\vec{k}) = 0, \tag{10}$$

where $f(\vec{k}) = \sum_j e^{i\vec{k}\cdot\vec{T}_j}$ is the summation running over the six lattice translation vectors $\vec{T}_j$ connecting the central cell to the six nearest-neighbor cells in the graphene lattice. Evaluating the sum, we get the result

$$f(\vec{k}) = 2\cos(\sqrt{3}k_x a) + 4\cos(\sqrt{3}k_x a/2)\cos(3k_y a/2), \tag{11}$$

where $a$ is the bond length. Inverting Eq. (10) for a given Bloch momentum $\vec{k}$, we get the result

$$\bar{k}a = \cos^{-1}[3^{-1}(3 + f(\vec{k}))^{1/2}], \tag{12}$$

which yields the band structure energy $E(\vec{k}) = \hbar^2\bar{k}^2/(2m)$. We note here that in the low energy limit ($\bar{k}a \ll 1$), Eq. (12) leads to the same result as the nearest-neighbor tight-binding theory, viz.,

$$E - E_0 = \pm t\sqrt{3 + f(\vec{k})}, \tag{13}$$

where $E_0 = \hbar^2 m^{-1} a^{-2}$ and $t = \hbar^2(3ma^2)^{-1}$.

Alternatively, the linear equations, Eq. (6), may be cast as an eigenvalue problem. Expressing $\vec{b}$ in terms of $\vec{a}$, one can rewrite the linear equations as

$$[SB^{-1}SB]\vec{b} = \lambda\vec{b}, \tag{14}$$

where the matrix product on the left hand side is a function of $\vec{k}$ only and $\lambda = \exp(-2i\bar{k}a)$. Omitting the trivial solution $\lambda = 1$ in the eigenvalue problem, one finds the equation that yields the remaining two eigenvalues: $\lambda^2 - \lambda(g(\vec{k}) - 1) + 1 = 0$, with $g(\vec{k}) = (3 + 4f(\vec{k}))/9$, the solution of which yields the same band structure energy as Eq. (12).

For a given $\vec{k}$, Eq. (12) yields multiple bands due to the multi-valued solutions of the arc cosine function, corresponding to the low lying as well as the higher-energy states. The low-energy band structure obtained from Eq. (12) is plotted in Fig. 2, which clearly shows the well-known linear dispersion of the graphene bands at the Brillouin zone corner points $K$ and $K'$.

The linear dispersion can be obtained by a small momentum expansion of Eq. (12) around the $K$ or $K'$ point, $\vec{k} = \vec{K} + \vec{q}$, where $\vec{K} = (4\pi(3\sqrt{3}a)^{-1}, 0)$ and $\vec{q}$ is small. The result is

$$\bar{k} = 2^{-1}q \pm (2a)^{-1}\pi, \tag{15}$$

with the corresponding energy

$$E = \frac{\pi^2\hbar^2}{8ma^2} \pm \hbar v_F q, \tag{16}$$

where the Fermi velocity is $v_F = (3/8)^{1/2}\,\pi\hbar(2ma)^{-1}$, and the ± sign corresponds to the upper (lower) band forming the Dirac cone. A comparison with the density-functional result,[5] where $v_F = 8.2 \times 10^5$ m/s, yields the effective electron mass of $m/m_e = 0.78$. Fig. (3) shows the computed density of states, which shows the well known van Hove singularities for graphene and the linear density of states near the Dirac point.

*Chiral Wave Functions* – The wave functions corresponding to a specific solution $\bar{k}(\vec{k})$ in the Brillouin zone

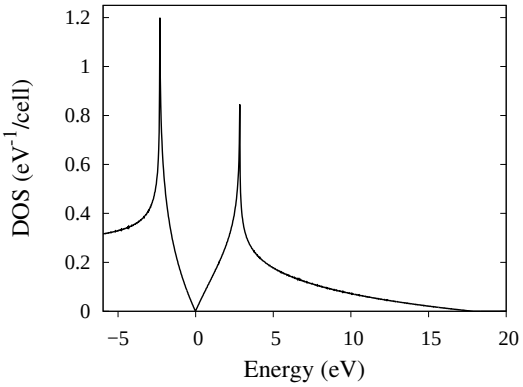


FIG. 3. Density of states for the graphene lattice, corresponding to the solution, Eq. (12), with the energy of the Dirac point defined as zero.

are obtained by using the standard Gaussian elimination and back substitution method to solve the set of linear equations $M\vec{X} = 0$, Eq. (6). Focusing on the solutions close to the Brillouin zone corner points $K$ and $K'$, we reduce the matrix $M$ to the upper triangular form, take the arbitrary coefficient $b_3$ to be of the form $b_3 = \alpha + \beta q$, where $\alpha$ and $\beta$ are constants and the lowest order terms in the small-$q$ expansion have been kept, and use the back substitution to find the result

$$\vec{X}_K(\vec{q}) = \begin{pmatrix} a_1 \\ a_2 \\ a_3 \\ b_1 \\ b_2 \\ b_3 \end{pmatrix} = \begin{pmatrix} g\cos\zeta_+ \\ g^*\cos\zeta_- \\ \cos\zeta \\ ig\sin\zeta_- \\ ig^*\sin\zeta_+ \\ i\sin\zeta \end{pmatrix} + O(q^2), \qquad (17)$$

where $g = \exp(i2\pi/3)$, $\zeta = \gamma/2 + \pi/4$, $\zeta_\pm = \zeta \pm 2\pi/3$, and $\gamma = \tan^{-1}(q_y/q_x)$ as defined in Fig. 1. Note that the phase shifts appearing in the trigonometric part of the coefficients are shifted for each wire in the unit cell by $4\pi/3$ relative to each other. The amplitudes of the wave function for the two sublattices may be obtained from the propagating solutions on one of the wires using Eq. (1). For example, in terms of the the wave functions on the first wire, we have

$$\begin{pmatrix} \psi_A \\ \psi_B \end{pmatrix}_K = \begin{pmatrix} a_1 + b_1 \\ a_1 e^{i\bar{k}a} + b_1 e^{-i\bar{k}a} \end{pmatrix}. \qquad (18)$$

Substituting the coefficients from the expression for $\vec{X}_K(\vec{q})$, Eq. (17), it is straightforward to show that this can be cast in the pseudo-spin form: $(\psi_A, \psi_B) = (\cos(\theta/2), \sin(\theta/2)e^{i\phi})$, with the spinor pointing along along $(\theta, \phi)$. After renormalization, we readily find

$$\begin{pmatrix} \psi_A \\ \psi_B \end{pmatrix}_K = \frac{1}{\sqrt{2}} \begin{pmatrix} e^{i\gamma/2} \\ \pm e^{-i\gamma/2} \end{pmatrix} \qquad (19)$$

where +(-) refers to the upper (lower) band. Proceeding similarly for the $K'$ point, we find

$$\begin{pmatrix} \psi_A \\ \psi_B \end{pmatrix}_{K'} = \frac{1}{\sqrt{2}} \begin{pmatrix} e^{-i\gamma/2} \\ \mp e^{i\gamma/2} \end{pmatrix} \qquad (20)$$

These solutions correspond precisely to the chiral wave functions in graphene. For states in the vicinity of $K$, we have $\theta = \pi/2$ and $\phi = -\gamma$ or $\phi = -\gamma + \pi$, for the upper and the lower band, respectively. Similarly for $K'$, we have $\phi = \gamma$ or $\phi = \gamma + \pi$, so that the chirality is switched between $K$ and $K'$.

These ideas can be extended to other situations such as the finite graphene lattices, e. g., the graphene nanoribbons and carbon nanotubes. We consider below the states produced by an isolated vacancy in graphene as another illustration of the method. The vacancy in graphene has been of considerable interest because of the possibility of it being a magnetic center,[11,13] in spite of the fact that there is no magnetic atom present.

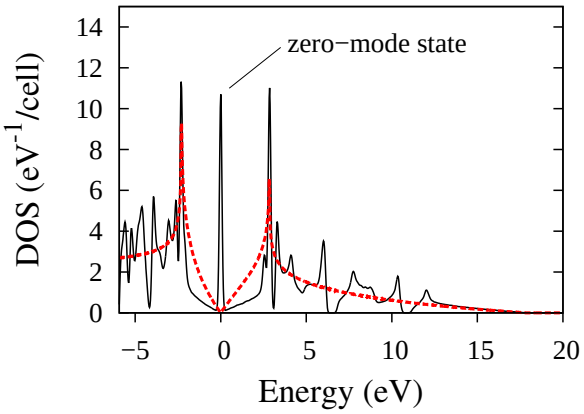


FIG. 4. (Color online) Density of states for the graphene lattice with a vacancy obtained from the supercell calculation (black line) compared to the same without the vacancy (red dashed line). The vacancy-induced zero mode states appear as a $\delta$-function peak at the Dirac point energy $E = 0$ as discussed in the text.

*Vacancy states* – According to the so called "zero mode theorem," originally due to Lieb[12] (and rediscovered in the literature with alternative proofs[13,14]): In a bipartite lattice with nearest-neighbor tight-binding interaction, the number of zero mode states is at least $N = |N_A - N_B|$, where $N_A(N_B)$ are the number of occupied $A(B)$ sublattice sites. In the context of the graphene lattice with a vacancy, the theorem immediately leads to a single zero-mode state at the Dirac point energy, which has been discussed in detail in the literature.[13,14] In a periodic supercell structure with a single vacancy in the supercell, the zero mode theorem leads to a flat band at the Dirac point energy and consequently to a $\delta$-function peak at zero energy in a density-of-states plot.[13]

We have studied the vacancy states using the present method for a $3 \times 3$ supercell containing a single vacancy in the supercell. The resulting linear equations similar to

Eq. (6) were solved numerically and the results are shown in the density of states plot in Fig. (4), which clearly shows the presence of the zero-mode states at the Dirac point energy. In addition to the zero-mode states, the two peaks due to the van Hove singularities in the original graphene bands are seen in the supercell results as well; the other peaks and valleys are specific to the finite supercell used and would not be present in the infinite graphene lattice with a single vacancy (See, for example, Ref.[13] ).

In summary, we presented a new way of describing the electronic structure of graphene. The method is not limited to graphene, but can be extended to other periodic crystalline structures as well. The simplest application is for the electronic structure of a single band solid as was illustrated for graphene, but the method may be developed to generalize to multi-band systems. The method might have advantages over other methods in many situations such as transport through graphene nanoribbons, where reflection and transmission coefficients may be computed directly. Furthermore, our work suggests new ways of constructing Dirac band materials through nanopatterning techniques.

This research was supported by the U.S. Department of Energy, Office of Basic Energy Sciences, Division of Materials Sciences and Engineering under Award No. DE-FG02-00ER45818.

[1] A. H. Castro Neto, F. Guinea, N. M. R. Peres, K. S. Novoselov, and A. K. Geim, "The electronic properties of graphene," Rev. Mod. Phys. **81**, 109 (2009).

[2] D. S. L. Abergel, V. Apalkov, J. Berashevich, K. Ziegler, and T. Chakraborty, "Properties of Graphene: a theoretical perspective," Adv. Phys. **59** 261 (2010).

[3] S. Das Sarma, S. Adam, E. H. Hwang, and E. Rossi, "Electronic transport in two-dimensional graphene," Rev. Mod. Phys. **83**, 407 (2011).

[4] P. R. Wallace, "The band theory of graphite," Phys. Rev. **71**, 622 (1947).

[5] See, for example, B. R. K. Nanda and S. Satpathy, "Strain and electric field modulation of the electronic structure of bilayer graphene," Phys. Rev. B **80**, 165430 (2009).

[6] C.-H. Park and S. G. Louie, "Making massless Dirac fermions from a patterned two-dimensional electron gas," Nano Lett. **9**, 1793 (2009).

[7] J. S. Griffith, "A free-electron theory of conjugated molecules," Trans. Faraday Soc. **49**, 345 (1953).

[8] J.-B. Xia, "Quantum waveguide theory for mesoscopic structures," Phys. Rev. B **45** 3593 (1992).

[9] A. M. Jayannavar and P. Singha Deo, Phys. Rev. B **49**, 13685 (1994).

[10] S. Mishra and S. Satpathy, "Fiber-mesh photonic molecule," Optics Comm. **281**, 1077 (2008).

[11] R. R. Nair, M. Sepioni, I-Ling Tsai, O. Lehtinen, J. Keinonen, A. V. Krasheninnikov, T. Thomson, A. K. Geim and I. V. Grigorieva, "Spin-half paramagnetism in graphene induced by point defects," Nature Phys. **8**, 199 (2012).

[12] E. H. Lieb, "Two Theorems on the Hubbard Model," Phys. Rev. Lett. **62**, 1201 (1989).

[13] B. R. K. Nanda, M. Sherafati, Z. Popovic, and S. Satpathy, "Electronic structure of the substitutional vacancy in graphene: Density-functional and Green's function studies," New J. Physics **14**, 083004 (2012); Erratum: **15**, 039501 (2013).

[14] V. M. Pereira, J. M. B. Lopes dos Santos, and A. H. Castro Neto, "Modeling disorder in graphene," Phys. Rev. B **77**, 115109 (2008).